

Cite this: DOI: 10.1039/c0lc00555j

www.rsc.org/loc

High-speed droplet generation on demand driven by pulse laser-induced cavitation

Sung-Yong Park,^{*a} Ting-Hsiang Wu,^b Yue Chen,^a Michael A. Teitell^c and Pei-Yu Chiou^{*a}

Received 2nd November 2010, Accepted 6th January 2011

DOI: 10.1039/c0lc00555j

We report on a pulse laser-driven droplet generation (PLDG) mechanism that enables on-demand droplet generation at rates up to 10 000 droplets per second in a single-layer PDMS-based microfluidic device. Injected droplet volumes can be continuously tuned between 1 pL and 150 pL with less than 1% volume variation.

Digital microfluidic devices have attracted great interest for lab-on-chip applications. By isolating aqueous droplets containing biological or biochemical contents in an immiscible oil medium, cross-contamination between droplets is eliminated, and reagents can be transported without dispersion. A variety of applications have been demonstrated, including chemical and biochemical screening,^{1,2} enzyme kinetic assays,^{3,4} polymerase chain reaction (PCR),^{5,6} protein crystallization,⁷ and nanoparticle or organic molecule synthesis.^{8,9}

In these digital microfluidic devices, the ability for high-speed droplet generation with precise volume control plays an important role in realizing high throughput and quantitative analyses. Passive-type flow-focusing devices are commonly used to achieve high-speed droplet generation.^{10,11} For example, Yobas *et al.* utilized a flow-focusing geometry in a silicon-based device to demonstrate highly uniform emulsion droplet generation at a speed of thousands of droplets per second.¹² However, it is difficult to achieve on-demand droplet generation in these passive-type devices.

To achieve droplet generation on demand, active control valves need to be integrated into fabricated microfluidic devices. Zeng *et al.* have shown a pneumatically driven, microvalve-integrated device for on-demand droplet generation.¹³ In this device, a pneumatic pump deforms a thin PDMS membrane between top and bottom microchannels to control the on/off valve switching time, droplet size, and production rate. A speed of 100 droplets per second has been demonstrated with droplet volumes ranging from 1.3 nL to 13.3 nL and volume variation from 7.2% to 1.6%, respectively. Hsiung *et al.* designed a microfluidic chip capable of chopping a stream of

dispersed phase using a movable PDMS wall structure actuated by external air pressure.¹⁴ This device enables on-demand droplet generation at a speed of 20 droplets per second and droplet size from 10 μm to 120 μm in diameter. However, these and most other previously demonstrated active-type devices either have a much slower droplet generation speed compared with passive-type devices or relatively poor droplet volume uniformity at high generation speeds.^{15–18}

Here, we present a high-speed, pulse laser-driven droplet generation (PLDG) mechanism that enables on-demand droplet generation at rates up to 10 000 droplets per second with precise volume control in a single-layer PDMS microfluidic device without any additional on-chip mechanical pumps or valves.

A schematic of the PLDG device is illustrated in Fig. 1. It consists of two microchannels, one water and one oil, connected by a nozzle-shaped opening and fabricated by standard soft-lithography techniques.¹⁹ The dimensions of both channels are 100 μm in width and 100 μm in height. The neck of the nozzle is 30 μm in width. A stable water–oil interface is formed at the junction by properly adjusting the flow rates of water and oil.

The actuation mechanism of PLDG is based on laser pulse induced, rapidly expanding cavitation vapor bubbles. When an intense laser pulse is focused in a liquid medium such as water, the

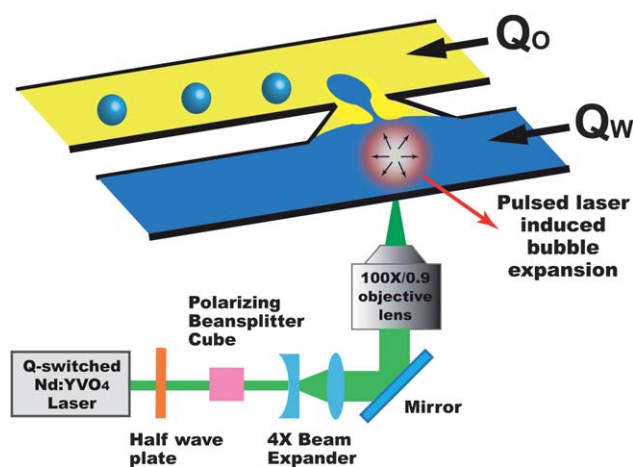


Fig. 1 Schematic of the PLDG device that consists of two microfluidic channels connected by a nozzle-like opening. A highly focused intense laser pulse induces a rapidly expanding cavitation bubble to push the nearby water into the oil channel for droplet formation.

^aDepartment of Mechanical and Aerospace Engineering, University of California at Los Angeles (UCLA), 43-147 Eng. IV, 420 Westwood Plaza, Los Angeles, CA, 90095-1597, USA. E-mail: pychiou@seas.ucla.edu; spark5@ucla.edu; Fax: +1-310-206-4830; Tel: +1-310-825-8620

^bDepartment of Electrical Engineering, UCLA, USA

^cDepartments of Pathology and Pediatrics, California NanoSystems Institute, Broad Stem Cell Research Center, Jonsson Cancer Center, and Molecular Biology Institute, UCLA, 4-762 MRL, 675 Young Drive South, Los Angeles, CA, 90095-1732, USA. E-mail: MTeitell@mednet.ucla.edu; Fax: +1-310-267-0382; Tel: +1-310-206-6754

strong optical field induces water molecule breakdown which generates a hot plasma at the focal point.^{20–22} The heat quickly dissipates into the medium and creates a rapidly expanding cavitation bubble to perturb the stable oil–water interface and push the neighboring water into the oil channel to form aqueous droplets. The lifetime of a bubble from laser excitation to collapse is bubble size dependent and varies from tens to hundreds of microseconds in our experiments.

To induce cavitation bubbles, a Q-switched Nd:YVO₄ pulsed laser beam (EKSPILA, Jazz 20) with a wavelength of 532 nm, 15 ns pulse width, and a maximum repetition rate of 100 kHz was focused through an objective lens (100×, NA 0.9) into the pulsed channel. This high-speed laser-induced droplet generation process was captured by a custom built time-resolved imaging system.²³ A flashlamp (Nanolite, High-Speed Photo-Systeme) is used to provide illumination pulses with exposure times as short as 14 ns and was synchronized with a CCD camera (AxioCam MRm, Zeiss) and the laser. LabVIEW (National Instruments) programming enables our control of the number of laser pulses, the interval between pulses, and the delay time to trigger the flashlamp.

Fig. 2 presents captured time-resolved images that show the droplet formation process with PLDG. Corn oil for a continuous oil phase and a phosphate-buffered saline (PBS) buffer for a dispersed aqueous phase were used in all experiments. Before a laser pulse, the water and oil flow rates were adjusted to form a stable interface at the nozzle-shaped opening (Fig. 2(a)). Then, a bubble was excited within 1 μs after the arrival of a laser pulse (Fig. 2(b)). The expanding bubble pushed water into the oil channel (Fig. 2(c)) and reached its maximum size at 3–5 μs and started to collapse (Fig. 2(d)). During the bubble collapse process, a neck-shaped connection was created between the droplet and the water channel (Fig. 2(e–g)). When the unstable neck-shaped connection was broken, a 137 pL droplet was generated by a 100 μJ laser pulse in 500 μs and transported away in the oil channel (Fig. 2(h and i)).

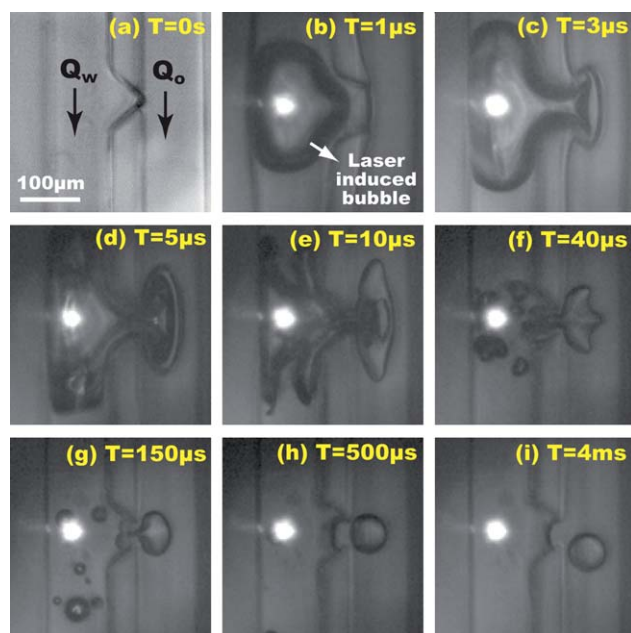


Fig. 2 Time-resolved images of on-demand droplet generation using PLDG. A 137 pL droplet is generated by a 100 μJ laser pulse at $Q_w = 12 \text{ mL h}^{-1}$ and $Q_o = 0.2 \text{ mL h}^{-1}$.

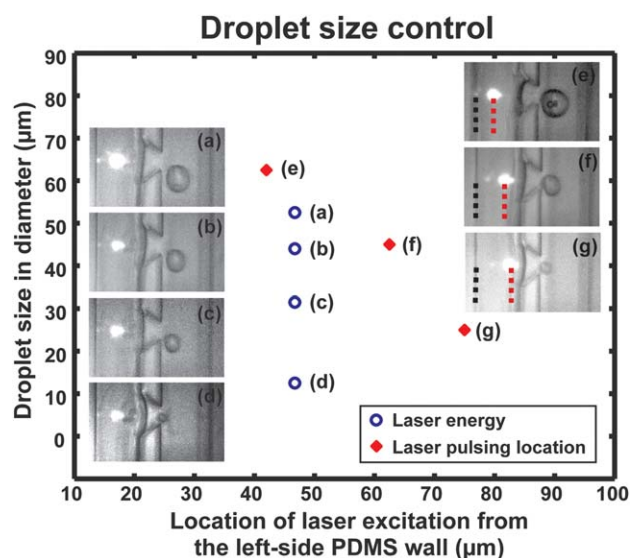


Fig. 3 Droplet size control by tuning the laser energy with (a) 100 μJ, (b) 90 μJ, (c) 80 μJ, and (d) 70 μJ at a pulsing location 47 μm away from the PDMS wall, and by varying the location of laser excitation at (e) 41 μm, (f) 62.5 μm, and (g) 75 μm away from the PDMS wall with a fixed 100 μJ pulsing energy.

The volume of the injected droplets can be tuned either by adjusting the pulse laser energy or the laser excitation location. Fig. 3(a–d) show the pulse energy-tuned droplet volume control. The pulsing location is fixed at 47 μm away from the left PDMS channel wall and the pulse energy is tuned by a beam polarizer from 100 μJ to 70 μJ. Since the pulse energy determines the bubble size, a higher energy pulse generates a larger water droplet. Fig. 3(e and f) show the pulsing location-dependent droplet volume control with a fixed pulse energy of 100 μJ. Laser pulsing close to the oil–water interface produces small volume droplets. By controlling the pulse energy and pulsing location, we can tune the injected droplet volume from 1 pL to 150 pL.

A computer-controlled setup using LabVIEW 6.5 controls the number of laser pulses and the interval between each laser pulse. Fig. 4 shows continuous droplet generation with various laser pulsing intervals from 2 ms to 100 μs. On-demand droplet generation as fast as 10 000 droplets per second has been achieved using PLDG (see Fig. 4(d)). One of the factors limiting the current droplet generation speed is the flow rate in the oil channel, which needs to be fast enough to remove a droplet before the next droplet is generated to prevent droplet merging at higher generation speeds. Higher droplet

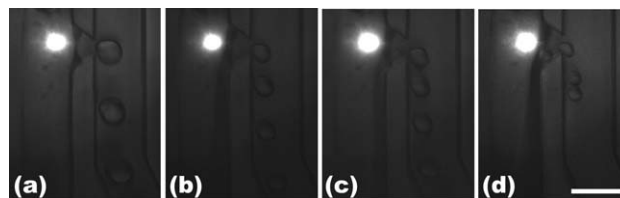


Fig. 4 Continuous droplet generation with varied laser pulsing intervals, (a) 2 ms at $Q_w = 44 \text{ mL h}^{-1}$ and $Q_o = 1.2 \text{ mL h}^{-1}$, (b) 1 ms at $Q_w = 60 \text{ mL h}^{-1}$ and $Q_o = 2.4 \text{ mL h}^{-1}$, (c) 500 μs at $Q_w = 120 \text{ mL h}^{-1}$ and $Q_o = 4 \text{ mL h}^{-1}$, and (d) 100 μs at $Q_w = 190 \text{ mL h}^{-1}$ and $Q_o = 6.5 \text{ mL h}^{-1}$. In case (d), three laser pulses are used to demonstrate a droplet generation rate of 10 000 droplets per second. The scale bar is 100 μm.

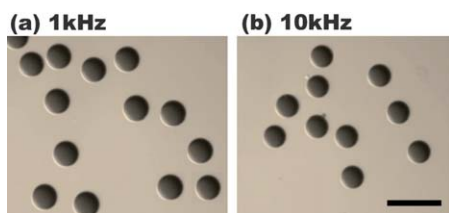


Fig. 5 Droplets were continuously generated at (a) 1 kHz and (b) 10 kHz laser pulsing frequencies. Droplets were then collected in dishes for volume uniformity analysis. The scale bar is 100 μm .

generation speeds are achievable with smaller droplets or higher oil flow speeds.

Droplet volume uniformity is very important in many lab-on-chip applications, especially for quantitative analyses. To evaluate droplet uniformity, droplets with colored dyes were produced under conditions used in Fig. 4(b and d), followed by collection in a dish (Fig. 5). The image processing toolbox in Matlab 7.1 was used to analyze the collected droplet volume variation by taking cross-sectional images. The injected droplets showed less than 1% volume variation.

Our microfluidic device reliability has been tested by continuously pulsing the water channel with 100 μJ pulses at a 1 kHz repetition rate for 1 hour, corresponding to 3.6 million bubble generation cycles. No damage was observed on the device.

To conclude, we present a pulse laser-driven droplet generation (PLDG) mechanism that enables high-speed droplet generation on demand with precise and tunable volume control on a single-layer PDMS microfluidic device without any extra on-chip mechanical pumps or valves. On-demand droplet formation using PDLG is realized by a pulse laser-induced bubble expansion that perturbs a stable oil–water interface. We have experimentally demonstrated on-demand droplet generation at a speed of 10 000 droplets per second. Droplets with a tunable volume between 1 pL and 150 pL have been generated either by adjusting the laser pulse energy or pulsing location. Droplet volume variations of less than 1% have been estimated at both 1 kHz and 10 kHz repetition rates. Device reliability testing has shown no observable damage after continuous laser pulsing for 3.6 million bubble generation cycles. As such, PDLG provides a powerful approach for high-throughput and quantitative digital biochemical analyses.

Acknowledgements

This project is supported by a NSF Career Award (ECCS 0747950), NSF DBI-0852701, NSF ECCS 0901154, a UC Discovery Bioscience

Biotechnology Award (#178517), the NIH Roadmap for Medical Research Nanomedicine Initiative (PN2EY018228), the Eli and Edythe Broad Center of Regenerative Medicine and Stem Cell Research at UCLA Innovation Award, and the Prostate Cancer Foundation Challenge Award.

References

- 1 E. Brouzes, M. Medkova, N. Savenelli, D. Marran, M. Twardowski, J. B. Hutchison, J. M. Rothberg, D. R. Link, N. Perrimon and M. L. Samuels, *Proc. Natl. Acad. Sci. U. S. A.*, 2009, **106**, 14195–14200.
- 2 J. Clausell-Tormos, D. Lieber, J.-C. Baret, A. El-Harrak, O. J. Miller, L. Frenz, J. Blouwolff, K. J. Humphry, S. Köster, H. Duan, C. Holtze, D. A. Weitz, A. D. Griffiths and C. A. Merten, *Chem. Biol. (Cambridge, MA, U. S.)*, 2008, **15**, 427–437.
- 3 A. Huebner, M. Srisa-Art, D. Holt, C. Abell, F. Hollfelder, A. J. deMello and J. B. Edel, *Chem. Commun.*, 2007, 1218–1220.
- 4 L. S. Roach, H. Song and R. F. Ismagilov, *Anal. Chem.*, 2005, **77**, 785–796.
- 5 W. Li, H. H. Pham, Z. Nie, B. MacDonald, A. Genter and E. Kumacheva, *J. Am. Chem. Soc.*, 2008, **130**, 9935–9941.
- 6 Y.-H. Chang, G.-B. Lee, F.-C. Huang, Y.-Y. Chen and J.-L. Lin, *Biomed. Microdevices*, 2006, **8**, 215–225.
- 7 B. T. C. Lau, C. A. Baitz, X. P. Dong and C. L. Hansen, *J. Am. Chem. Soc.*, 2007, **129**, 454.
- 8 L.-H. Hung, K. M. Choi, W.-Y. Tseng, Y.-C. Tan, K. J. Shea and A. P. Lee, *Lab Chip*, 2006, **6**, 174–178.
- 9 T. Hatakeyama, D. L. Chen and R. F. Ismagilov, *J. Am. Chem. Soc.*, 2006, **128**, 2518–2519.
- 10 J. F. Edd, D. Di Carlo, K. J. Humphry, S. Köster, D. Irimia, D. A. Weitz and M. Toner, *Lab Chip*, 2008, **8**, 1262–1264.
- 11 M. Joanicot and A. Ajdari, *Science*, 2005, **309**, 887–888.
- 12 L. Yobas, S. Martens, W.-L. Ong and N. Ranganathan, *Lab Chip*, 2006, **6**, 1073–1079.
- 13 S. Zeng, B. Li, X. Su, J. Qin and B. Lin, *Lab Chip*, 2009, **9**, 1340–1343.
- 14 S.-K. Hsiung, C.-T. Chen and G.-B. Lee, *J. Micromech. Microeng.*, 2006, **16**, 2403–2410.
- 15 R. Prakash, R. Paul and K. V. I. S. Kaler, *Lab Chip*, 2010, **10**, 3094–3102.
- 16 J. Gong and C.-J. Kim, *Lab Chip*, 2008, **8**, 898–906.
- 17 J. Xu and D. Attinger, *J. Micromech. Microeng.*, 2008, **18**, 065020.
- 18 F. Malloggi, S. A. Vanapalli, H. Gu, D. v. d. Ende and F. Mugele, *J. Phys.: Condens. Matter*, 2007, **19**, 462101.
- 19 J. C. McDonald, D. C. Duffy, J. R. Anderson, D. T. Chiu, H. Wu, O. J. A. Schueller and G. M. Whitesides, *Electrophoresis*, 2000, **21**, 27–40.
- 20 R. Dijkink and C.-D. Ohla, *Lab Chip*, 2008, **8**, 1676–1681.
- 21 A. Vogel, S. Busch and U. Parlitz, *J. Acoust. Soc. Am.*, 1996, **100**, 148–165.
- 22 R. K. Chang, J. H. Eickmans, W.-F. Hsieh, C. F. Wood, J.-Z. Zhang and J.-b. Zheng, *Appl. Opt.*, 1988, **27**, 2377–2385.
- 23 T.-H. Wu, L. Gao, Y. Chen, K. Wei and P.-Y. Chiou, *Appl. Phys. Lett.*, 2008, **93**, 144102.